Fracture Mechanics of Concrete and Concrete Structures - Assessment, Durability, Monitoring and Retrofitting of Concrete Structures- B. H. Oh, et al. (eds)
ⓒ 2010 Korea Concrete Institute, Seoul, ISBN 978-89-5708-181-5

3D FE analysis of fasteners at elevated temperatures

G. Periškić, J. Ožbolt & R. Eligehausen
Institute of Construction Materials, University of Stuttgart, Stuttgart, Germany

ABSTRACT: In the present paper the results of 3D FE investigation on headed studs at elevated temperatures are presented. For modeling of concrete under fire conditions a thermo-mechanical model (Ožbolt et al. 2005, 2008) is used. In the parametric FE analysis of single headed stud anchors loaded in tension, the influence of embedment depth, heating time, edge distance and number of surfaces exposed to heating was investigated. In case of anchor groups the influence of embedment depth, anchor spacing and heating time was examined. The results of the FE analysis show that the resistance of single anchors and anchor groups with large edge distance under fire conditions are primarily dominated by embedment depth. Anchors with small embedment depth are very sensitive to fire and may even fail under design load. In case of small edge distance and multiple sides heating of the concrete body the anchor resistance is additionally affected by edge distance.

1 INTRODUCTION

Concrete does not burn, however, when its temperature increases for a couple of hundred of degrees Celsius its behavior changes significantly. The concrete mechanical properties, such as strength, elasticity modulus and fracture energy, are at high temperatures rather different than for concrete at normal temperature. At high temperature large temperature gradients lead in concrete structures to temperature induced stresses which cause damage. Furthermore, creep and relaxation of concrete due to high temperature play also important role. The main reason for the complexity of the behavior of concrete at high temperature is due to the fact that concrete contains water, which changes its aggregate state. Moreover, the aggregate can change its structure or it can lose its weight through the emission of CO_2, such as calcium based stones. Although the behavior of concrete at high temperature is in the literature well documented (Anderberg & Thelandersson 1976, Schneider 1988, Bažant & Kaplan 1996, Khoury 2006), further tests are needed to clarify the tensile post-peak behavior of concrete, which has significant influence on the response of concrete structures. The main problem in the experimental investigations is due to the fact that such experiments are rather demanding, i.e. one has to perform loading and measurement at extremely high temperatures. Furthermore, such experiments can be carried out only on relatively small structures. To better understand behavior of concrete structures, as an alternative to experiments one can employ numerical analysis. However, one needs models, which can realistically predict behavior of concrete at high temperature.

In the present paper a three-dimensional (3D) model based on the thermo-mechanical coupling between mechanical properties of concrete and temperature is employed. The microplane model is used as isothermal constitutive law for concrete whose model parameters are made temperature dependent. The model is implemented into a three-dimensional finite element code and its performance is first compared with the experimental results known from the literature. Subsequently, the influence of high temperature on the pullout concrete cone resistance of headed stud anchors is investigated. The finite element analysis is performed in two steps. For given temperature boundary conditions (air temperature and, or, concrete surface temperature) calculated distribution of temperature is calculated. In the second step the required load history is applied with taking into account the influence of temperature on the concrete mechanical properties.

2 TRANSIENT THERMAL ANALYSIS

As the first step of coupling between mechanical properties of concrete and temperature, the temperature distribution over a solid structure of volume Ω at time t is calculated. In each point of continuum, which is defined in Cartesian coordinate system (x,y,z), the conservation of energy has to be fulfilled. This can be expressed by the following equation:

$$\lambda \Delta T(x,y,z,t) - c\rho \frac{\partial T}{\partial t}(x,y,z,t) = 0 \tag{1}$$

where T = temperature [K], λ = conductivity [W/mK], c = heat capacity [J/kgK], ρ = mass density [kg/m^3] and Δ = Laplace-Operator. The surface boundary condition that has to be satisfied reads:

$$\lambda \frac{\partial T}{\partial \mathbf{n}} = \alpha (T_M - T) \tag{2}$$

where $\mathbf{n}$ = normal to the boundary surface Γ, α = transfer or radiation coefficient [W/(m^{2}K)] and T_M = temperature of the media in which surface Γ of the solid Ω is exposed to [K] (for instance temperature of air). To solve the problem by the finite element method the above Equations 1, 2 have to be written in weak (integral) form (Ožbolt et al. 2005, 2008).

3 DECOMPOSITION OF STRAIN

In the present model the total strain tensor ε_{ij} (indicial notation) for stressed concrete exposed to high temperature can be decomposed as:

$$\varepsilon_{ij} = \varepsilon_{ij}^{m}(T, \sigma_{kl}) + \varepsilon_{ij}^{ft}(T) + \varepsilon_{ij}^{lits}(T, \sigma_{kl}) \tag{3}$$

where ε_{ij}^{m} = mechanical strain tensor, ε_{ij}^{ft} = free thermal strain tensor, ε_{ij}^{lits} = load-induced thermal strain tensor (Ožbolt et al. 2005, 2008).

In general, the mechanical strain component can be decomposed into elastic, plastic and damage part. In the present model these strain components are obtained from the constitutive law. The free thermal strain is stress independent and is experimentally obtained by measurements on the load-free specimen. In such experiments it is not possible to isolate shrinkage of concrete, therefore the temperature dependent shrinkage is contained in the free thermal strain. The load-induced thermal strain is stress and temperature dependent. It appears only during the first heating and not during subsequent cooling and heating cycles (Khoury 2006). This strain is irrecoverable and can cause severe tensile stresses during cooling in concrete structures. It generally comprises several components including transient strain (consisting of transitional thermal creep and drying creep), time-dependant creep and changes in elastic strain that occur during heating under load (Khoury 2006). Due to the fact that these components have similar properties – they are all irrecoverable – and are hard to be individually identified in an experiment, it is common praxis to model them mutually in a single strain tensor. The same method is used in the present model.

3.1 *Mechanical strain*

The mechanical strain components are obtained from the constitutive law of concrete. In the present model temperature dependent (isothermal) microplane model is used as constitutive law (Ožbolt et al. 2001). In the microplane model the material is characterized by a relation between the stress and strain components on planes of various orientations. These planes may be imagined to represent the damage planes or weak planes in the microstructure, such as those that exist at the contact between aggregate and the cement matrix. In the model the tensorial invariance restrictions do not need to be directly enforced. Superimposing the responses from all microplanes in a suitable manner automatically satisfies them. The microplane model used in the present paper was proposed by Ožbolt et al. (2001). The temperature dependency of the microplane model is adopted such that the macroscopic properties of concrete (Young's modulus, compressive and tensile strength and fracture energy) are made temperature dependent, according to the available experimental data (Zhang & Bićanić 2002, Schneider 1988).

3.2 *Free thermal strain*

The experimental evidence (Schneider 1988) indicates that the free thermal strains in concrete specimen mainly depend on the type and amount of the aggregate. Although the experiments indicate that the free thermal strain depends on the rate of the temperature, in the present model it is assumed that this strain depends only on temperature. Moreover, it is assumed that in the case of a stress free specimen, the thermal strains are equal in all three mutually perpendicular directions (isotropic thermal strains). The temperature dependency of the free thermal strain, as adopted in the present model, reads:

$$\dot{\varepsilon}_{ij}^{ft} = \alpha \dot{T} \delta_{ij}$$
$$\alpha = \begin{cases} \dfrac{6.0\ 10^{-5}}{7.0 - \theta} & for\ 0 \le \theta \le 6 \\ 0 & for\ 0 \le \theta \le 6 \end{cases} \tag{4}$$

with

$$\theta = \left(T - T_0\right) / 100°C \tag{5}$$

3.3 *Load-induced thermal strain*

When a concrete specimen is first loaded and subsequently exposed to high temperature, the resulting thermal strain is different than for the case of an unloaded specimen (Thelandersson 1974, Khoury 2006). The difference can be obtained if the free thermal strain is subtracted from the resulting thermal strain, which results in the so called load-

induced thermal strain. It is relatively insensitive to aggregate type and cement paste since it originates in a common gel or C-S-H structure. Due to its similarity for different concrete types, a common 'master' LITS cure is taken to exist up to temperatures of about 450°C (Khoury 2006). In the present model the bi-parabolic function is used for representing load induced thermal strain (Nielsen et al. 2002), which reads:

$$\dot{\varepsilon}^{tm}(T,\sigma) = \frac{\sigma}{f_c^{T_0}} \beta \dot{T}$$

$$\beta = 0.01 \cdot \begin{Bmatrix} 2 \cdot A \cdot \theta + B & for\ 0 \le \theta \le \theta^* = 4.5 \\ 2 \cdot C \cdot (\theta - \theta^*) + 2 \cdot A \cdot \theta^* + B & for\ \theta > \theta^* \end{Bmatrix} \quad (6)$$

where θ^* is a dimensionless transition temperature between the two expressions (470°C) and θ according to Equation 5. The above two expressions are introduced to account for abrupt change in behavior detected in the experiments. A, B and C are experimentally obtained constants that are in the present model set as: $A = 0.0005$, $B = 0.00125$ and $C = 0.0085$.

3.4 *Reinforcement modeling at high temperature*

To realistically model the behavior of reinforced concrete at high temperatures, it is necessary to properly reproduce the behavior of concrete as well as to take into account the influence of temperature on the performance of reinforcement.

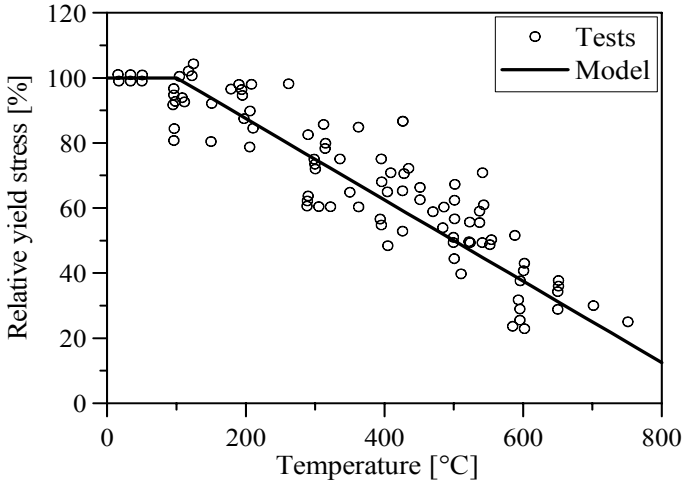

Figure 1. Relative yield stress as function of temperature – test results (Kordina & Meyer-Ottens 1981) and model assumption.

In the present model discrete modeling of reinforcement with 1-dimensional elements is used, assuming perfect bond between steel and concrete. According to experimental results, high temperature has very strong influence on the behavior of steel, causing significant reduction of its mechanical properties. To account for this influence, simple bi-linear temperature dependant functions for degradation of Young's modulus and yield strength are assumed in the model. Figures 1, 2 show adopted model assumptions as well as experimental results (Kordina & Meyer-Ottens 1981).

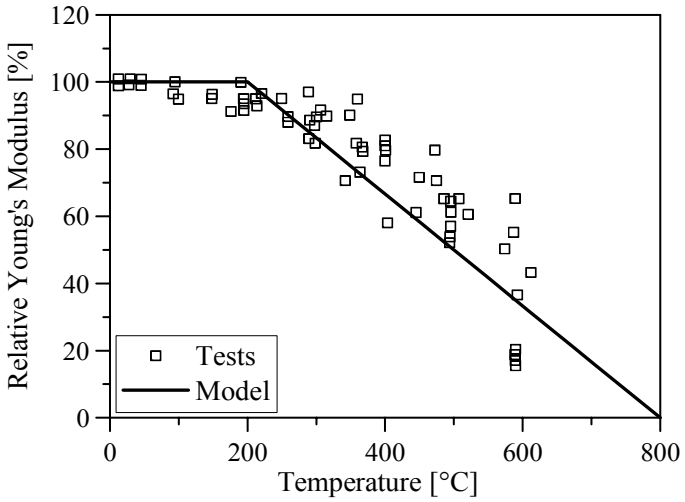

Figure 2. Relative Young's Modulus as function of temperature – test results (Kordina & Meyer-Ottens 1981) and model assumption.

4 NUMERICAL ANALYSIS OF HEADED STUDS AT HIGH TEMPERATURE

The main goal of the performed numerical analysis is to investigate the behavior of headed studs loaded in tension under fire conditions, principally regarding concrete cone failure mode. Three different cases are investigated: single anchors without edge influence (edge distance $c \ge 10h_{ef}$), single anchors close to an edge and anchor groups without edge influence. For each case different embedment depths are analyzed: $h_{ef} = 50$, 100, 150 and 200 mm. The anchors are first loaded with admissible load assuming room temperature of 20°C (Equation 7). In the next step the fire at the anchor side of the specimen is simulated. The air heating temperature at the upper specimen side is taken according to ISO 833 (equivalent to DIN 4102 part 2, Equation 8). If no failure occurrs during heating, the anchor is subsequently pulled out from the concrete block for the following load histories: (i) 30 minutes after start of heating, (ii) 90 minutes after start of heating and (iii) 120 minutes after start of heating. For comparison reasons a calculation without heating is also performed.

$$F_{adm.} = 8.1 \cdot \sqrt{f_{cc}} \cdot h_{ef}^{1.5} / 2.5 \quad (7)$$

$$T_{Air}(t) - T_{Air}(t_0) = 345\ log(8t + 1) \quad (8)$$

A typical FE Model is shown in Figure 3. For the discretisation of concrete 4-node solid elements are

applied while for steel 8-node solid elements are used. The contact between steel and concrete is modeled by interface elements, which are able to transfer only compression forces. To avoid crack appearance in the concrete body due to thermal strains, reinforcement is applied in tensile and compressive zone of the plate. The reinforcement cross section area in each zone is chosen to be 0.5 % of the plate cross section. The model is restrained in loading direction at the distance of $5h_{ef}$ from the anchor. The heated area around the anchor at the upper side of the concrete block has a radius of $r = 2.5h_{ef.}$ In this way no constrains were imposed in the heated area in order to avoid numerical difficulties. Moreover, the concrete cone is able to develop without constraint influence, being affected only by fire. To save computational time symmetry conditions are assumed, i.e. only one half of the geometry is modeled in case of anchors with edge influence (Fig. 3) and one quarter in case of single anchors and anchor groups without edge influence.

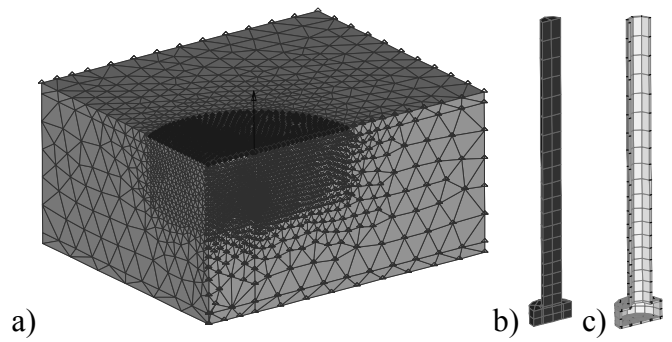

Figure 3. Typical FE mesh, symmetry assumed: concrete elements with boundary conditions (a), headed stud mesh (b) and interface elements (c).

The goal of the numerical study is to investigate concrete cone failure mode. To avoid steel failure linear-elastic behavior of the anchor with Young's modulus $E_s = 200\,000$ N/mm^2 and Poisson's ratio $\nu_s = 0.33$ is assumed. For reinforcement elements bilinear behavior with yield stress of $f_y = 500$ N/mm^2 is adopted. The concrete properties are taken as: Young's modulus $E_c = 28\,000$ N/mm^2, Poisson's ratio $\nu_c = 0.18$, tensile strength $f_t = 2.0$ N/mm^2, uniaxial compressive strength $f_c = 21.25$ N/mm^2 and concrete fracture energy $G_F = 0.065$ N/mm.

4.1 *Single anchors without edge influence*

Figures 4, 5 show calculated load-displacement curves for investigated load histories in case of anchors with embedment depths $h_{ef} = 50$ mm and $h_{ef} = 150$ mm, respectively. As expected, due to damage caused by thermal loading the pull-out resistance of the headed stud anchors is significantly reduced. It can be seen that with increase of temperature (heating time) the peak load and stiffness of the anchors decrease. Moreover, displacement at peak load significantly increases if the concrete member is exposed to fire. Compared to the initial resistance at $t = 0$ and $T_{Air} = 20$°C, the largest reduction of the ultimate load is obtained for the smallest embedment depth ($h_{ef} = 50$ *mm*) and for the second thermal loading history (90 min. heating). In this case the calculated ultimate load almost equals to the anchor's admissible load.

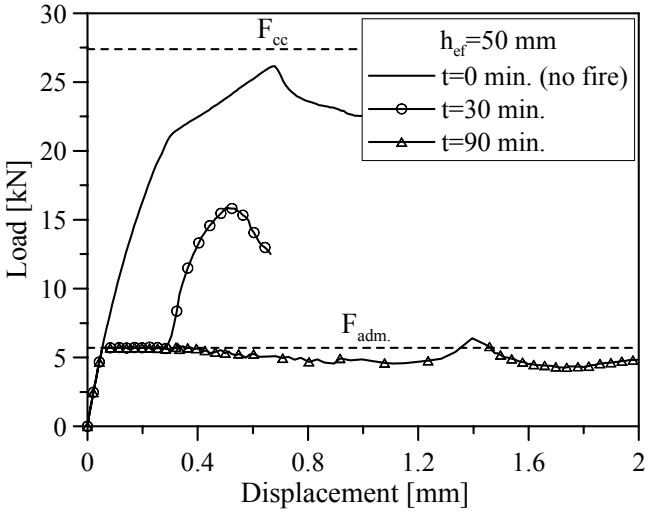

Figure 4. Load-displacement curves for the calculated load histories in case of anchor with $h_{ef} = 50$ mm.

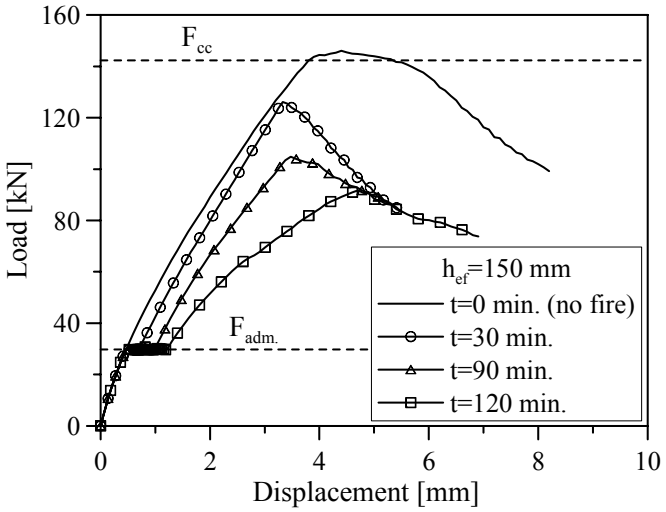

Figure 5. Load-displacement curves for the calculated load histories in case of anchor with $h_{ef} = 150$ mm.

Typical crack patterns for anchors with small ($h_{ef} = 50$ mm) and large ($h_{ef} = 150$ mm) embedment depth are shown in Figures 6, 7, respectively. The dark zone (maximal mechanical principal strain) shows localization of damage. It can be seen that for relatively small embedment depth the anchor lies over the entire length in the zone of very high temperature in which the concrete is almost completely destroyed. Extreme case is observed for embedment depth of $h_{ef} = 50$ mm and for the third loading history (120 min. of heating). For this case the ultimate pull-out capacity is smaller than the initially applied admissible load, i.e. the anchor fails during heating. The main reason for the failure is strong degradation

of concrete mechanical properties in the area close to the stud head as well as thermal induced cracking in concrete member.

For larger anchors and in case when the embedment depth is large compared to the thickness of a concrete member, the head of the stud lies in the zone of lower temperature. In this zone the concrete is less damaged. Consequently smaller ultimate load reduction is observed.

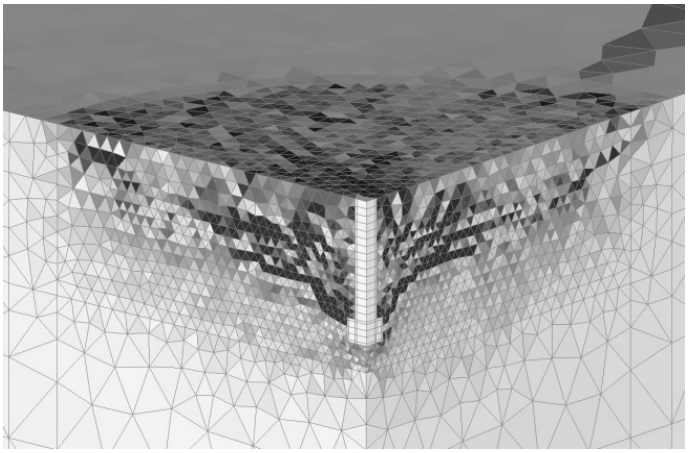

Figure 5. Typical crack pattern for anchors with small embedment depth – h_{ef} = 50 mm, t = 90 min.

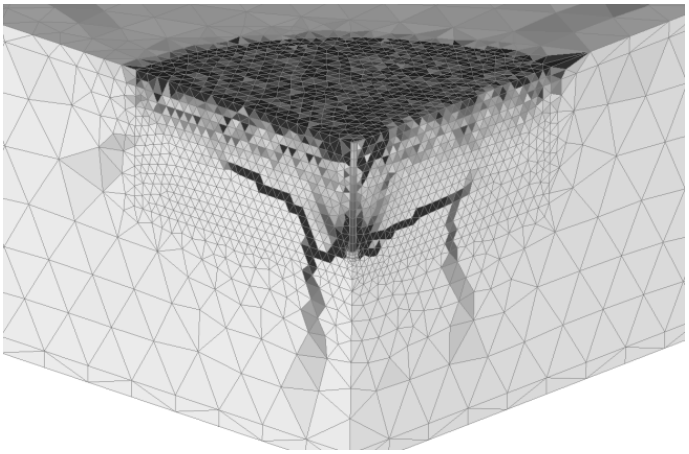

Figure 6. Typical crack pattern for anchors with large embedment depth – h_{ef} = 150 mm, t = 90 min.

In Figure 7 relative residual anchor capacity, defined as a ratio between the residual capacity at certain temperature $F_u(t)$ and the ultimate capacity without fire influence (at 20°C) F_u, is plotted as a function of heating time for different embedment depths. In case of h_{ef} = 50 mm and t = 120 min. the anchor fails during heating, therefore no capacity is plotted. Instead, an arrow is displayed, showing that the anchor capacity is lower than in case of t = 90 min. It can be clearly seen that embedment depth and heating time have dominant effects on the anchor capacity. With increasing heating time anchor capacity decreases. However, in case of large embedment depth the reduction of the anchor resistance is significantly lower (up to 10 % after t = 120 min.) than in case of small embedment depths.

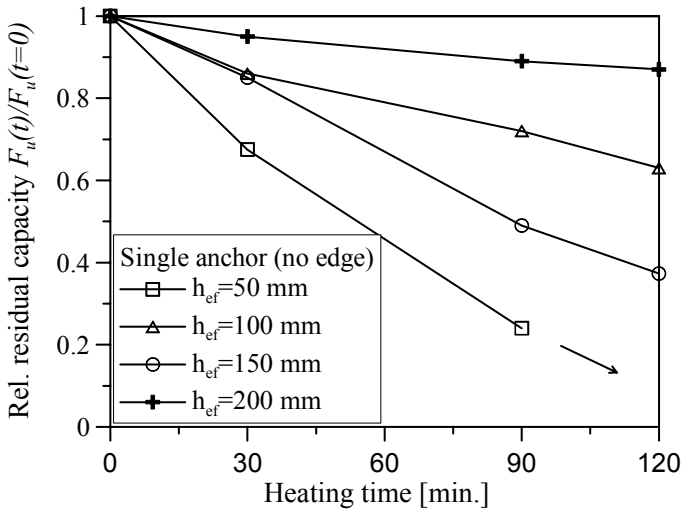

Figure 7. Relative residual capacity for single anchors without edge influence under fire as a function of heating time.

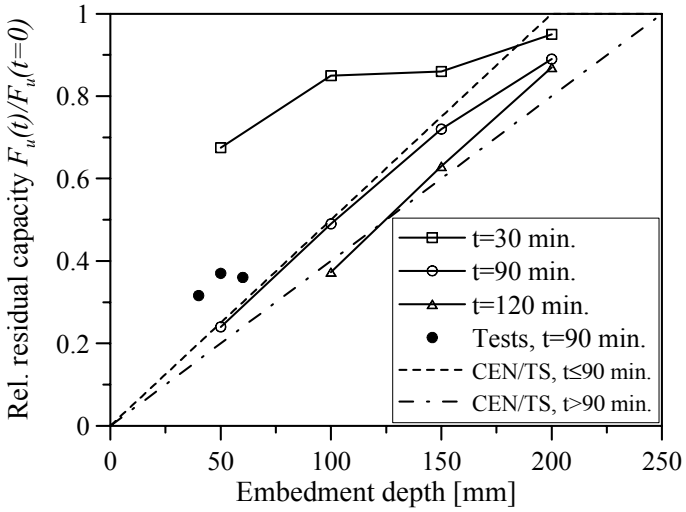

Figure 8. Relative residual capacity for single anchors without edge influence under fire as a function of embedment depth.

In Figure 8 calculated relative residual anchor capacity $F_u(t)/F_u$ is plotted as a function of embedment depth. In the same figure experimental results from Reick (2001) for embedment depths of h_{ef} = 40 *mm,* h_{ef} = 50 *mm* and h_{ef} = 60 *mm* after 90 min. of heating as well as predicted anchor capacity according to the current design code CEN/TS (2009) are shown. It can be seen, that the FE results for t = 90 min. and t = 120 min. show very good agreement with the design code. In case of 30 min. of heating the design code is clearly too conservative.

The experimental results from Reick (2001) show limited agreement with corresponding numerical results. This is probably due to different temperature distribution in the concrete member, i.e. in the FE analysis the air temperature on the concrete surface strictly follows the ISO 833 heating curve, which is in the first 10-15 minutes extremely steep, with gradients up to 300 °C/min. In practical applications it is rather difficult to achieve such steep temperature increase, therefore it can be expected that the actual temperature is somewhat lower than assumed in the

FE calculations. This results in slower heat flow into the concrete and consequently smaller reduction of concrete material properties. Furthermore, it can be seen that the test results from Reick (2001) do not follow the general trend of the numerical calculations and prediction of design code, i.e. that the relative anchor resistance increases with increasing embedment depth. This indicates that test results scatter significantly. It is well known that experimental measurements at high temperatures are rather demanding. Furthermore, the accuracy of the measurement equipment may be affected at high temperatures. The observed, partly limited agreement of experimental and numerical results is therefore acceptable.

4.2 *Single anchors with edge influence*

In case of anchors installed close to a concrete edge there are two possible configurations: i) single concrete surface is exposed to fire, such as in case of a slab and ii) 2 or more concrete surfaces are exposed to fire, as it would be the case for anchors installed in a column. Both cases were subject of FE investigation. Investigated geometry is similar to the case of anchors without edge influence, with edge distance on one side being reduced to 2 h_{ef}, 1 h_{ef} and 0.5 h_{ef}. Furthermore, the same discretization as in the previous case is employed.

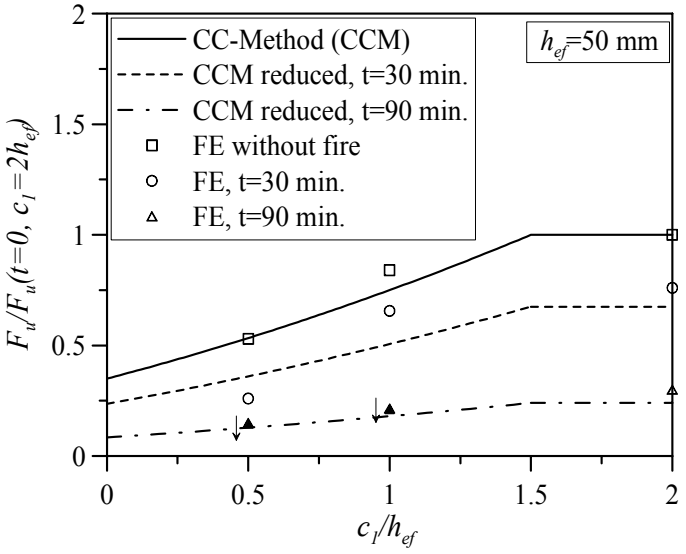

Figure 9. Relative residual capacity with reference to the case $c_1 = 2h_{ef}$ and $t = 0$ for single anchors with $h_{ef} = 50$ mm, edge influence and one-side heating as a function of c_1/h_{ef}.

Figures 9-11 show results of single side heated concrete block (i.e. slab-case) as a ratio between anchor residual capacity for edge distance c_1 and heating time t and anchor ultimate capacity for "large" edge distance ($c_1 = 2h_{ef} > c_{cr}$) without fire influence. In the same diagrams anchor ultimate strength according to CC-Method (Eligehausen et al. 2006) without fire influence as well as according to reduced CC-Method are shown. For the reduced CC-Method it was assumed that the reduction is equal to the reduction observed in the FE results for single anchors without edge influence (see Section 4.1. This allows effective comparison of residual capacities for anchors without and with edge influence.

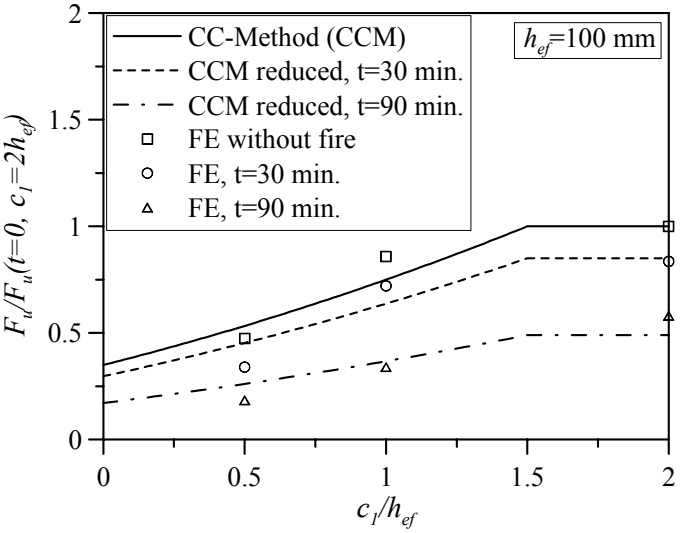

Figure 10. Relative residual capacity with reference to the case $c_1 = 2h_{ef}$ and $t = 0$ for single anchors with $h_{ef} = 100$ mm, edge influence and one-side heating as a function of c_1/h_{ef}.

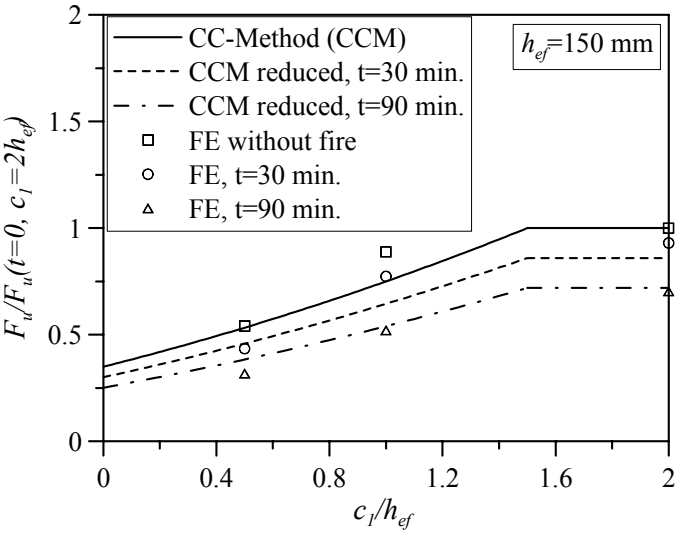

Figure 11. Relative residual capacity with reference to the case $c_1 = 2h_{ef}$ and $t = 0$ for single anchors with $h_{ef} = 150$ mm, edge influence and one-side heating as a function of c_1/h_{ef}.

The numerical results for the case without fire influence ($t = 0$) show good agreement with the CC-Method. Furthermore, for $t = 30$ min and $t = 90$ min. numerical results agree with reduced CC-Method. This means that the anchors close to an edge, when heated from one side only, behave similar to the anchors without edge influence. The anchor capacity reduction is large for small anchors and decreases with increasing anchor size. The main influencing parameter is embedment depth, anchor edge distance has no additional influence on the anchor capacity in case of fire conditions.

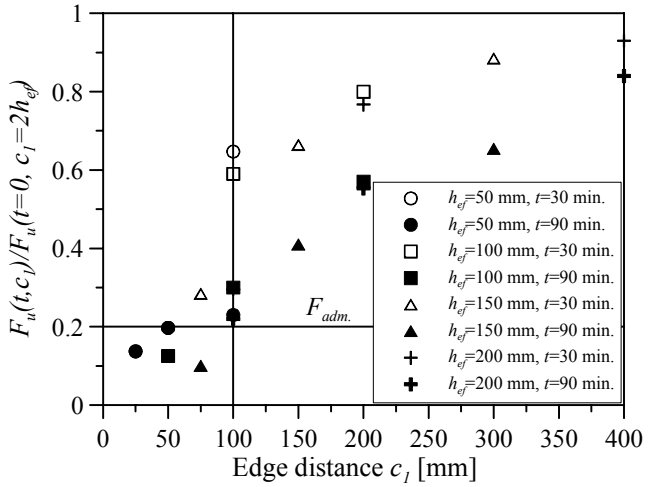

Figure 12. Relative residual capacity with reference to the case $c_1 = 2h_{ef}$ and $t = 0$ for single anchors with edge influence and multiple-side heating as a function of edge distance c_1.

Different behavior can be observed in case of multiple sides heating. In the present paper the case with heating from the "fastening side" and from the "closest edge side" is considered. In Figure 12 the ratio of the anchor residual resistance for certain heating time and edge distance $F_u(t,c_1)$ and ultimate resistance at "large" edge distance ($c_1 = 2h_{ef} > c_{cr}$) for $t = 0$ is plotted as a function of c_1 for different embedment depths. Corresponding relative admissible load is shown as well. It can be seen that for edge distances smaller than 100 mm anchors fail under admissible load before reaching 90 minutes of heating, even in the case of relative large embedment depth such as $h_{ef} = 150$ mm. With increasing edge distance relative residual resistance increases. The reason for this behavior is the fact that anchors close to the heated edge lie in the area of very high temperature, similar to anchors with small embedment depth in case of single side heating. Mechanical properties degradation as well as thermal induced cracking have negative influence on the capacity of such anchors.

According to the current design code (CEN/TS 2009), in case of spatial heating the minimal edge distance must be at least $c_{min} = 300$ mm or $c_{min} = 0.5h_{ef}$. The presented numerical results show that the minimal edge distance could be reduced to 100 mm. However, experimental results are needed to confirm this observation.

4.3 *Anchor groups without edge influence*

In the anchor group investigation under fire the focus is set on the group of 4 anchors. The heating is applied on one side only, since it is assumed that anchors are placed far from the concrete edge.

Results of the investigation are shown in Figures 13 to 15. Similar to the case of single anchors with edge influence, the relative residual anchor capacity $F_u(t)/F_u(s=4h_{ef},t=0)$ is plotted as a function of s/h_{ef} and compared to corresponding results of single anchors by the means of reduced CC-Method. As expected, the results for anchor groups are similar to those of single anchors. The main influencing factors are embedment depth and heating time. The reduction of the anchor capacity is strong for small embedment depths and decreases with increasing h_{ef}.

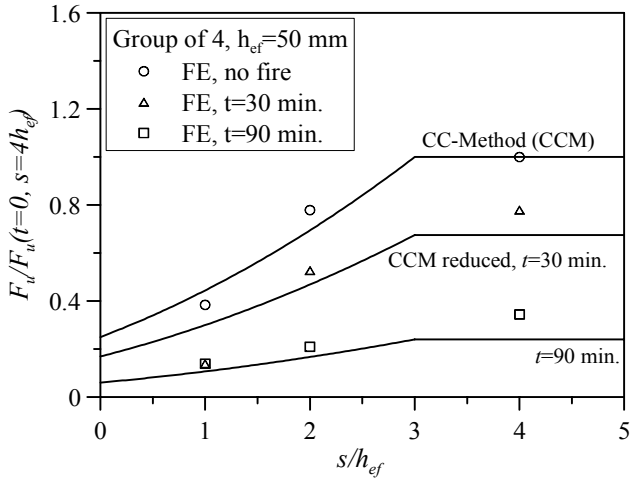

Figure 13. Relative residual capacity with reference to $s = 4h_{ef}$ and $t = 0$ for groups with $h_{ef} = 50$ mm as function of s/h_{ef}.

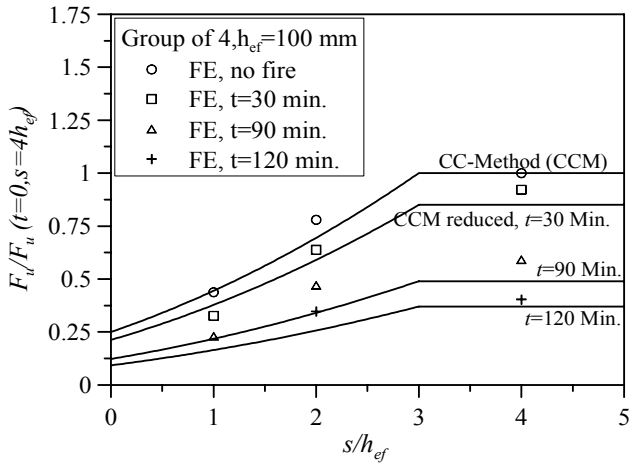

Figure 14. Relative residual capacity with reference to $s = 4h_{ef}$ and $t = 0$ for groups with $h_{ef} = 100$ mm as function of s/h_{ef}.

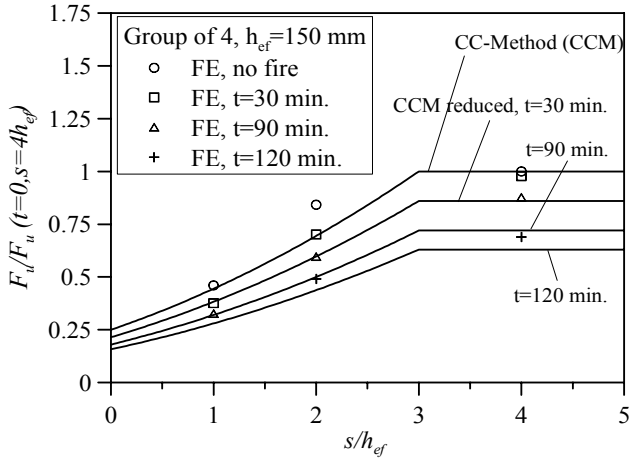

Figure 15. Relative residual capacity with reference to $s = 4h_{ef}$ and $t = 0$ for groups with $h_{ef} = 150$ mm as function of s/h_{ef}.

The critical anchor spacing under fire of 4 $h_{ef.}$, as assumed in the current design code (CEN/TS 2009), seems to be appropriate.

5 SUMMARY

In the present paper the influence of the heating of concrete on the capacity of single and multiple headed stud anchors is numerically investigated. The FE analysis is performed by the use of phenomenological thermo-mechanical model for concrete that is based on the temperature dependant microplane model (Ožbolt et al. 2005, 2008).

In case of single anchors without influence of concrete edge the relative anchor resistance at high temperature is mainly controlled by embedment depth and heating time. For small embedment depths the relative anchor resistance is strongly reduced, since the whole ancor is placed in the area of high temperature. With increasing embedment depth the influence of temperature decreases. Furthermore, the relative anchor resistance decreases with growing heating time. The results show that headed studs under admissible load with 50 mm embedment depth fail after 90 minutes of heating. For anchors with 200 mm embedment depth no significant influence of high temperature after 90 minutes of heating is observed.

In case of anchors close to a concrete edge and heating from one side ("fastening side", no spatial heat flux) the relative anchor resistance decreases with increasing temperature. The magnitude of the reduction is similar to the case for anchors without influence of concrete edge. In case of single anchors and two-side heating ("fastening side" and "closest edge side") the edge distance has a significant influence on anchor resistance. The FE calculations show, that fastenings fail under admissible load, independent on their embedment depth, if edge distance is smaller than 100 mm. With increasing edge distance the influence of two-side heating decreases and becomes similar to the case with one-side heating.

Anchor groups without concrete edge influence behave similarly to single anchors without edge influence. The main influencing parameters are embedment depth and heating time.

Finally, it can be concluded that fastenings exhibit significant capacity reduction in case of fire. The main influencing factors on the ultimate anchor capacity are embedment depth, heating time and in some cases edge distance. The current design code is generally able to predict fastening capacity under high temperature, but in some cases it is too conservative. To verify the fastenings behavior in case of fire in more detail and to confirm presented numerical results experimental investigations should be performed.

REFERENCE

Anderberg, Y. & Thelandersson, S. 1976. Stress and deformation characteristics of concrete at high temperatures. *Bulletin 54.* Lund: Lund Institute of technology.

Bažant, Z.P. & Kaplan, M.F. 1996. *Concrete at High Temperatures: Material Properties and Mathematical Models*. Harlow: Longman.

Eligehausen, R., Mallée, R. & Silva, J.F. 2006. *Anchorage in Concrete Construction*. Berlin: Ernst & Sohn.

European Committee for Standardization (CEN). 2009. Design of fastenings for use in concrete. *Technical Specification*. Brussels: CEN.

Khoury, G.A. 2006. Strain of heated concrete during two thermal cycles – Parts 1,2 and 3. *Magazine of Concrete Research* 58: 367-385, 58: 387-400, 58: 421-435.

Kordina, K. & Meyer-Ottens, C. 1981. *Beton Brandschutz Handbuch*. Düsseldorf: Verlag Bau+Technik.

Nielsen, C.V., Pearce, C.J. & Bićanić, N. 2002. Theoretical model of high temperature effects on uniaxial concrete member under elastic restraint. *Magazine of Concrete Research* 54: 239-249.

Ožbolt, J., Li, Y.-J. & Kožar, I. 2001. Microplane model for concrete with relaxed kinematic constraint. *International Journal of Solids and Structures* 38: 2683-2711.

Ožbolt, J., Kožar, I., Eligehausen, R. & Periškić, G. 2005. Three-dimensional FE analysis of headed stud anchors exposed to fire. *Computers and Concrete* 2: 249-266.

Ožbolt, J., Periškić, G., Reinhardt, H.-W. & Eligehausen, R. 2008. Numerical analysis of spalling of concrete cover at high temperature. *Computers and Concrete* 5: 279-293.

Reick, M. 2001. *Brandverhalten von Befestigungen mit großem Randabstand in Beton bei zentrischer Zugbeanspruchung; Dissertation*. Stuttgart: Institut für Werkstoffe im Bauwesen, Universität Stuttgart.

Schneider, U. 1988. Concrete at High Temperatures – A General Review. *Fire Safety Journal* 13: 55-68.

Thelandersson, S. 1974. Mechanical behaviour of concrete under torsional loading at transient, high temperature conditions. *Bulletin 46*. Lund: Lund Institute of technology.

Zhang, B. & Bićanić, N. 2002. Residual Fracture Toughness of Normal- and High-Strength Gravel Concrete after Heating to 600°C. *ACI Materials Journal* 99: 217-226.